

RL-TR-96-2
Final Technical Report
February 1996



PLZT CERAMIC BASED ELECTRO-OPTIC BEAM STEERING DEVICE FOR OPTICAL INTERCONNECTION AND PATHWAY ADJUSTMENT

Syracuse University

Q. Wang Song

APPROVED FOR PUBLIC RELEASE; DISTRIBUTION UNLIMITED.

19960513 048

**Rome Laboratory
Air Force Materiel Command
Rome, New York**

DTIC QUALITY INSPECTED 1

This report has been reviewed by the Rome Laboratory Public Affairs Office (PA) and is releasable to the National Technical Information Service (NTIS). At NTIS, it will be releasable to the general public, including foreign nations.

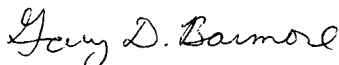
RL-TR- 96-2 has been reviewed and is approved for publication.

APPROVED:



RICHARD J. MICHALAK
Project Engineer

FOR THE COMMANDER:



GARY D. BARMORE, Major, USAF
Deputy Director of Surveillance & Photonics

If your address has changed or if you wish to be removed from the Rome Laboratory mailing list, or if the addressee is no longer employed by your organization, please notify Rome Laboratory/ (OCP), Rome NY 13441. This will assist us in maintaining a current mailing list.

Do not return copies of this report unless contractual obligations or notices on a specific document require that it be returned.

REPORT DOCUMENTATION PAGE

Form Approved
OMB No. 0704-0188

Public reporting burden for this collection of information is estimated to average 1 hour per response, including the time for reviewing instructions, searching existing data sources, gathering and maintaining the data needed, and completing and reviewing the collection of information. Send comments regarding this burden estimate or any other aspect of this collection of information, including suggestions for reducing this burden, to Washington Headquarters Services, Directorate for Information Operations and Reports, 1215 Jefferson Davis Highway, Suite 1204, Arlington, VA 22202-4302, and to the Office of Management and Budget, Paperwork Reduction Project (0704-0188), Washington, DC 20503.

1. AGENCY USE ONLY (Leave Blank)		2. REPORT DATE February 1996		3. REPORT TYPE AND DATES COVERED Final Feb 94 - Feb 95	
4. TITLE AND SUBTITLE PLZT CERAMIC BASED ELECTRO-OPTIC BEAM STEERING DEVICE FOR OPTICAL INTERCONNECTION AND PATHWAY ADJUSTMENT				5. FUNDING NUMBERS C - F30602-94-C-0041 PE - 62702F PR - 4600 TA - P3 WU - PW	
6. AUTHOR(S) Q. Wang Song					
7. PERFORMING ORGANIZATION NAME(S) AND ADDRESS(ES) Syracuse University Office of Sponsored Programs Skytop Office, Skytop Road Syracuse NY 13210				8. PERFORMING ORGANIZATION REPORT NUMBER N/A	
9. SPONSORING/MONITORING AGENCY NAME(S) AND ADDRESS(ES) Rome Laboratory/OCP 25 Electronic Pky Rome NY 13441-4515				10. SPONSORING/MONITORING AGENCY REPORT NUMBER RL-TR-96-2	
11. SUPPLEMENTARY NOTES Rome Laboratory Project Engineer: Richard J. Michalak/OCP/(315) 330-3150					
12a. DISTRIBUTION/AVAILABILITY STATEMENT Approved for public release; distribution unlimited.				12b. DISTRIBUTION CODE	
13. ABSTRACT (Maximum 200 words) An optical steering device based on a substrate of PLZT ceramic has been developed. On-substrate resistors were fabricated by evaporating a less conductive metal, and the resistance was controlled by varying the length of the metal film bar that connects two adjacent electrodes. A steering ability was experimentally demonstrated, which is in agreement with both the predicted estimation and the precise computer simulation. A fast time response and good beam quality were also observed. This device can have applications in laser disk tracking and/or fine alignment of board-to-board optical interconnections. To decrease the applied voltage, this PLZT substrate with large quadratic electro-optic coefficients should be used. The steering range achieved by this design is relatively small, but it is a continuous steering. When combined with a discrete steering device such as a blazed grating, a large steering range can be achieved.					
14. SUBJECT TERMS Electro-optics, PLZT, Beamsteering, Optical interconnects				15. NUMBER OF PAGES 36	
				16. PRICE CODE	
17. SECURITY CLASSIFICATION OF REPORT UNCLASSIFIED	18. SECURITY CLASSIFICATION OF THIS PAGE UNCLASSIFIED	19. SECURITY CLASSIFICATION OF ABSTRACT UNCLASSIFIED	20. LIMITATION OF ABSTRACT UL		

Table of Content

1. Introduction
2. Physical and electro-optic properties of PLZT ceramic
3. Design considerations
4. Device fabrication
5. Mathematical description of the electro-optic process
6. Experimental test of the device
7. Computer simulations
8. Discussions and conclusions

1. Introduction

Optical beam steering has a wide range of applications in optical memory, optical communication, and free space interconnections. For example in optical disk readout beam steering for autotracking is required to achieve vibration tolerance. In board-to-board optical interconnections small angle beam steering can be used to fine align the connecting beams after the boards are packaged, and large angle beam steering can make reconfigurable optical pathways to allow free space data transport among different data ports. A variety of techniques¹⁻⁷ to implement optical beam steering have been reported by means of electro-mechanical, acousto-optic and electro-optic effects. Mechanical beam steering methods are slow, inaccurate, and usually bulky. Acousto-optical beam steering is relatively expensive. In addition, its response time and angular resolution are not compatible with requirements. Electro-optical beam steering provides a motionless way to re-orient the beam's pathway, thus having the advantages of low weight, long life and fast time response. Previous electro-optic implementations of beam steering elements were based upon changing the refractive index of bulk electro-optic materials with triangular electrodes made on their top and bottom surfaces.⁸ Optical phased array beam steering implemented in multichannel lithium tantalate⁹ and lithium niobate crystals¹⁰ were reported. Techniques were also demonstrated to achieve electrically addressable liquid crystal prisms.¹¹

Lanthanum-modified lead zirconate titanate (PLZT) is a material demonstrating a strong quadratic electro-optic effect. In comparison with electro-optical crystals, PLZT has a larger electro-optical coefficient and is less expensive. When compared with liquid crystals, PLZT offers better physical stability and faster time response for practical applications. The fabrications of variable focal length lenses and dual focal point lenses with transparent electrodes on PLZT have been reported.¹²⁻¹⁴ These lenses use external resistive networks to produce the required voltage distribution. Optical shutters¹⁵⁻¹⁷ were also successfully demonstrated with PLZT. The high-efficiency phase grating structure¹⁷ can completely shut off the zero-order light with an applied voltage of 140 volts. The promising electro-optic properties of PLZT makes it possible to develop integrated electro-optical devices for optical beam steering and interconnection reconfiguration. Designs and computer simulations of PLZT-based electro-optic phased-array scanners^{18,19} have been reported. Based on phased array blazed grating scheme a programmable diffractive optical element performing selective beam steering²⁰ has been fabricated.

Most previous implementations of beam control devices utilize external sources to provide desired voltage distribution for the electrodes. They need complex wirings. Thus they are prone to malfunctions and are difficult to package for practical applications. As far as we know on-substrate resistive circuit fabrication producing the desired voltage distribution among the electrodes was only demonstrated on a liquid crystal structure.²¹ In this contract, PLZT based optical steering device was to be fabricated and demonstrated. Rather than using the transverse electro-optic effect^{18,19} we choose the longitudinal electro-optic effect. This choice makes the fabricated device almost independent of the

polarization of the incident laser beam because the field is determined by the voltage between the electrode and ground and thus is along the light path. Both sides of the PLZT wafer were used so that the electro-optic interaction length was equal to the thickness of the PLZT substrate. Transparent electrodes and the voltage distributing resistors were fabricated on the top surface while a transparent ground terminal was made on the bottom surface. The result is a compact device with only two external electrical connections. Experimental measurement and detailed simulations were conducted.

The content of this final report will be as follows. Section 2 briefs the basic properties of the PLZT ceramic wafer, followed by the design considerations and the fabrication implementation of a compact PLZT based electro-optic beam steering device in sections 3 and 4. Section 5 shows the mathematical process describing the electro-optical effect within the PLZT wafer when an external voltage is applied on the device. Section 6 presents the experimental tests of the fabricated device and section 7 explains the computer simulation. And finally, section 8, raises discussions and concludes the report.

2. Physical and electro-optic properties of PLZT ceramic

The index of refraction of an optical material can be generally expressed in the following mathematical form

$$\left(\frac{1}{n_1^2(x,y)}\right)x^2 + \left(\frac{1}{n_2^2(x,y)}\right)y^2 + \left(\frac{1}{n_3^2(x,y)}\right)z^2 + \left(\frac{1}{n_4^2(x,y)}\right)yz + \left(\frac{1}{n_5^2(x,y)}\right)zx + \left(\frac{1}{n_6^2(x,y)}\right)xy = 1, \quad (1)$$

provided that the z dimension is small as compared with those of the x and y . When x , y and z are chosen to be the optical axes of the material the last three terms on the left of the equation will vanish. PLZT is polycrystalline, which is prepared from PLZT powder by hot press in a temperature more than 1000°C . It can be prepared in any size or shape. Without an external field PLZT exhibits an isotropic optical property, with an intrinsic refractive indices of $n_1(x,y) = n_2(x,y) = n_3(x,y) = n_0 = 2.5$, and $n_4(x,y) = n_5(x,y) = n_6(x,y) = 0$. PLZT ceramic is quite transparent for a large range of wavelength. But due to its high intrinsic refractive index PLZT wafer has an intrinsic transmittance of 67% caused by its surface reflections.²² With proper anti-reflection coating on the surface, the transmittance can be increased as high as 98%.

PLZT has large quadratic electro-optic coefficients. When PLZT is placed in an electrical field, its index of refraction changes according to the following principle

$$\begin{bmatrix} \Delta \left(\frac{1}{n_1^2(x,y)} \right) \\ \Delta \left(\frac{1}{n_2^2(x,y)} \right) \\ \Delta \left(\frac{1}{n_3^2(x,y)} \right) \\ \Delta \left(\frac{1}{n_4^2(x,y)} \right) \\ \Delta \left(\frac{1}{n_5^2(x,y)} \right) \\ \Delta \left(\frac{1}{n_6^2(x,y)} \right) \end{bmatrix} = \begin{bmatrix} R_{11} & R_{12} & R_{12} & 0 & 0 & 0 \\ R_{12} & R_{11} & R_{12} & 0 & 0 & 0 \\ R_{12} & R_{12} & R_{11} & 0 & 0 & 0 \\ 0 & 0 & 0 & R_{44} & 0 & 0 \\ 0 & 0 & 0 & 0 & R_{44} & 0 \\ 0 & 0 & 0 & 0 & 0 & R_{44} \end{bmatrix} \begin{bmatrix} E_x^2(x,y) \\ E_y^2(x,y) \\ E_z^2(x,y) \\ E_y(x,y)E_z(x,y) \\ E_z(x,y)E_x(x,y) \\ E_x(x,y)E_y(x,y) \end{bmatrix}, \quad (2)$$

where R_{ij} indicates the quadratic electro-optic (Kerr) coefficients. When taking the electrical field direction as the x -axis, the index change can be simplified as

$$\Delta n_x(x, y) = -\frac{1}{2} n_0^3 R_{11} E^2(x, y), \quad (3)$$

$$\Delta n_y(x, y) = -\frac{1}{2} n_0^3 R_{12} E^2(x, y), \text{ and} \quad (4)$$

$$\Delta n_z(x, y) = -\frac{1}{2} n_0^3 R_{12} E^2(x, y), \quad (5)$$

where Δn_x , Δn_y and Δn_z refer to the refractive index changes when the polarization of the light is parallel to the electrical field direction and the other two perpendicular to the electrical field and each other. For the polarization which makes an arbitrary angle, $\theta(x, y)$, with the applied electrical field the refractive index change can be deduced by the following formula

$$\frac{1}{n^2(\theta(x, y))} = \frac{\cos^2(\theta(x, y))}{n_x^2(x, y)} + \frac{\sin^2(\theta(x, y))}{n_z^2(x, y)}. \quad (6)$$

PLZT's electro-optic coefficient can be different if the lanthanum concentration changes. As in our case PLZT 9/65/35 was used. This material has a 65/35 ratio of PbZrO_3 to PbTiO_3 with a lanthanum concentration of 9%. Numerical values of the Kerr coefficients in the literature¹²⁻¹³ are $R_{11} = 4.00 \times 10^{-16} \text{ m}^2/\text{V}^2$ and $R_{12} = -2.42 \times 10^{-16} \text{ m}^2/\text{V}^2$.

3. Design considerations

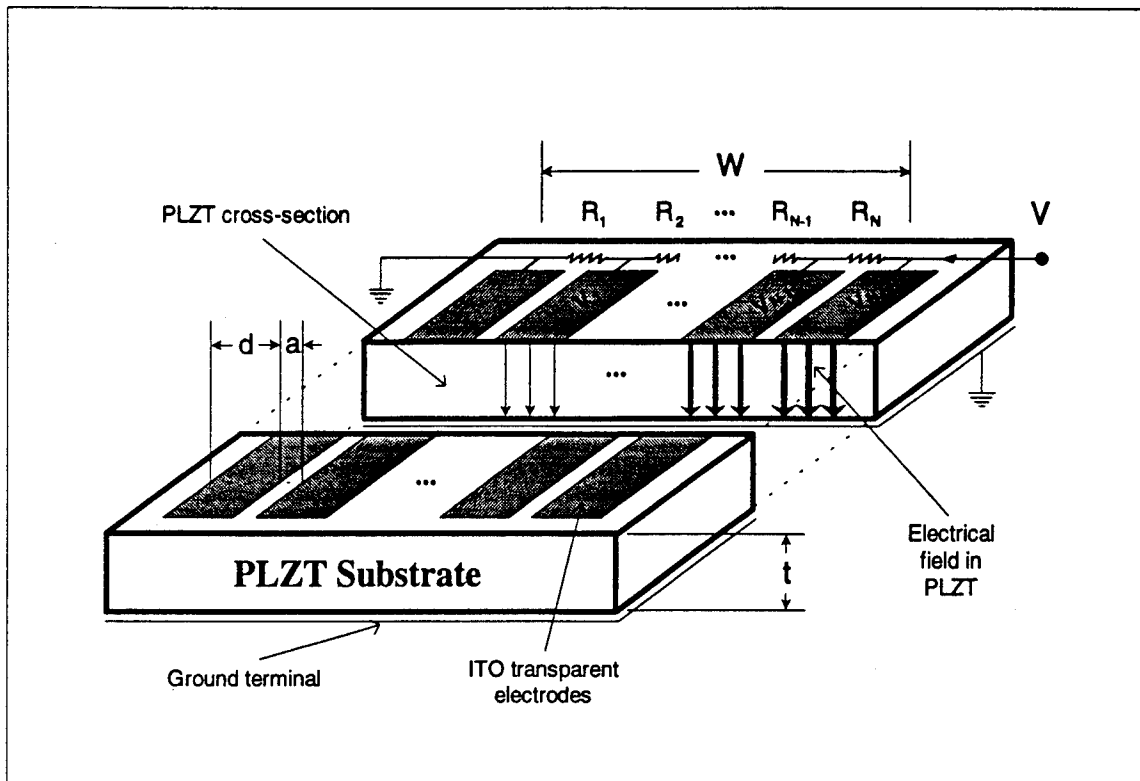


Figure 1. Three-dimensional view of the PLZT-based electro-optic steering device.

Figure 1 shows the three-dimensional view of the designed electro-optic beam steering device. The major electrical elements are distributed on the top surface of the electro-optic substrate. The structure consists of a series of electrodes and resistors and metal contacts to a voltage supply. The electrodes, which are shown as the shadowed parallelograms in the figure, are used to produce the designed electrical field in the PLZT substrate. The resistors, as indicated in the upper portion of the figure, are connected in series to provide the voltage distribution among the electrodes. A transparent conductive film, which serves as ground for the resistor network, is on the bottom surface of the PLZT substrate. Approximate mathematical expressions are used here to estimate the requirement for the resistors and predict the steering angle. A more precise derivation that

involves solving a two-dimensional Laplace equation and the index ellipsoid of the electro-optic effect in the PLZT ceramic will be presented in *Mathematical description of the electro-optic process* in Section 5.

Because of the transverse nature of the device operation the induced change in refractive index of the PLZT is

$$\Delta n = \frac{1}{2} n_0^3 R_{12} E^2, \quad (7)$$

no matter how the polarization is unless the laser light beam is incident normally onto the surface of the PLZT wafer. There are $N+1$ electrodes on the device, with the 0-th one connected to the ground. The N resistors between the electrodes produce a desired voltage distribution among the electrodes and thus the spatial electric field and the induced index distribution. An electrically controlled optical beam steering device is obtained in this fashion. In order to produce a linear index distribution across PLZT, the index modulation beneath the m -th electrode should be proportional to m , i.e.

$$\Delta n|_m = \frac{1}{2} n_0^3 R_{12} \left(\frac{V_m}{t} \right)^2 \propto m, \quad m = 1, 2, \dots, N, \quad (8)$$

where t is the thickness of the PLZT substrate and V_m is the voltage difference between the m -th electrode and the ground terminal. This index change requires a voltage distribution

$$V_m \propto \sqrt{m} = \sqrt{m} V_1 \quad (9)$$

with $V_N = V$, the supply voltage. V_1 , the potential difference over the first resistor, is called the scan voltage.¹⁸ When a beam is transmitted through the substrate, the electro-optic interaction length is the same as the thickness of the substrate. The steering angle for such

a device, in terms of the supply voltage V or the scan voltage V_1 , is expressed, in the small angle approximation as

$$\theta = \frac{t}{W} \Delta n|_N = \frac{n_0^3 R_{12} V^2}{2tW} = \frac{n_0^3 R_{12} V_1^2}{2t(d+a)}, \quad (10)$$

where d and a are the width and the spacing of the electrodes as defined in Figure 1 and W is the effective width of the electro-optic steering device with $W=N(d+a)$. For a fixed device effective area and required steering angle, the applied voltage can be reduced by decreasing the thickness of the PLZT substrate.

The potential drop over each individual resistor is expressed as

$$\Delta V_m = V_m - V_{m-1} = (\sqrt{m} - \sqrt{m-1})V_1. \quad (11)$$

Because all the resistors are connected in series, the required resistance ratio is defined as

$$\frac{R_m}{R_1} = \frac{\Delta V_m}{\Delta V_1} = (\sqrt{m} - \sqrt{m-1}). \quad (12)$$

Since the requirement only concerns the relative values of the resistors, precise control over the resistance is not necessary as long as the ratio remains unchanged. However, the total effective resistance needs to be limited within some range. If the resistance is too low, the device consumes too much power. This may cause heat-related problems. On the other hand, the resistance cannot be too high either, or the parasitic resistance between the electrodes may influence the steering effect.

4. Device fabrication

Fabrication was done through photolithographic techniques. Two devices were fabricated. One had an electrode period of $100\mu\text{m}$ with the electrode width and the spacing between two adjacent electrodes being $60\mu\text{m}$ and $40\mu\text{m}$, respectively. The other had an electrode period of $40\mu\text{m}$ with the electrode width and the inter-electrode spacing being $24\mu\text{m}$ and $16\mu\text{m}$, respectively. The length of the electrodes was 3mm . Each device's active area was $3\text{mm} \times 3\text{mm}$.

These two devices were fabricated with transparent indium tin oxide (ITO) for the electrodes and chromium for resistors. A combination of chromium and aluminum was used to produce a semi-transparent ground terminal on the bottom surface of the PLZT substrate for fabrication convenience. This caused a transmittance loss, but did not sacrifice the properties we were seeking. For the best performance of a practical device, a transparent deposition such as ITO for the ground is recommended. A PLZT wafer of dimension $20\text{mm} \times 20\text{mm} \times 0.40\text{mm}$ was used as the substrate. The ITO thin film 130nm thick was applied to one side of the PLZT ceramic wafer through magnetron sputter deposition from ITO composite targets. This yielded a measured sheet resistivity of $47.7\Omega/\text{sq}$. Electrodes were patterned onto the ITO film through 5 to 1 photolitho printing and a subtractive process by using argon ion beam etching. To guarantee that there would be no ITO remains between the electrodes to disturb the voltage distribution, over-etching was adopted. The electrodes' resistance were further reduced by evaporating $0.1\mu\text{m}$ thick and $4\mu\text{m}$ wide aluminum strips onto the center of the ITO electrodes. The purpose of the strips is to shorten the RCA constant, and thus the time response, of the device. Note that

these opaque aluminum strips are much narrower than the ITO electrodes. Therefore, the optical transmittance of the electro-optic beam steering device is not noticeably reduced by them.

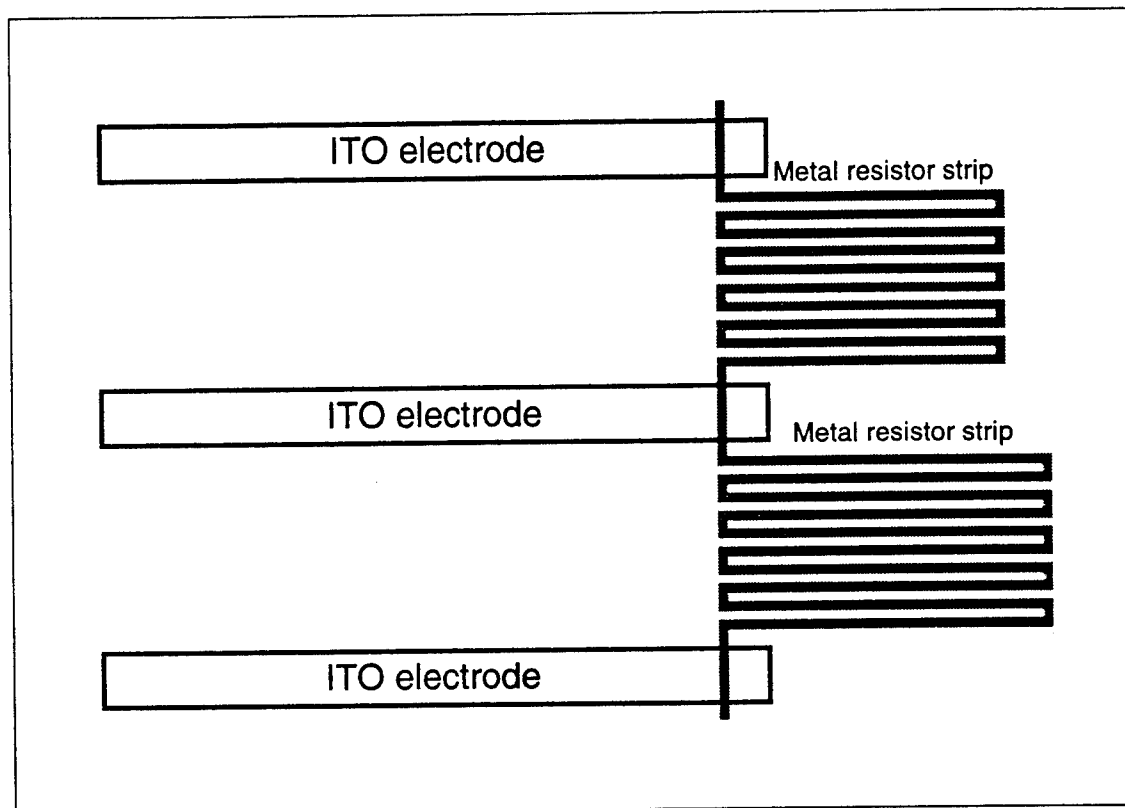


Figure 2. Illustration of chromium resistor patterning.

Figure 2 shows the resistant network patterning. The resistors were made of a thin film of a less conductive metal, chromium, through a thermal evaporation followed by a resist lift-off wet strip. A sheet resistivity of $103\Omega/\text{sq}$ was achieved by evaporating a chromium film of 50nm thickness. Each resistor was a $4\mu\text{m}$ wide chromium strip folded in a "square wave" pattern. The resistance of each resistor was controlled by varying its length

according to its designed value. The total resistance are $7.0 \text{ M}\Omega$ and $9.8 \text{ M}\Omega$ for the $40\mu\text{m}$ and $100\mu\text{m}$ period designs, respectively. The corresponding value for R_f are $808 \text{ k}\Omega$ and $1.79 \text{ M}\Omega$, respectively. The electrical field in PLZT varies along the direction perpendicular to the electrodes in a square root manner. Figure 1 also depicts the resulting field distribution with the stronger field denoted by thicker arrows. For simplicity, the inter-electrode field in this illustration has been ignored.

Two metal contacts were made and connected to the first and the last electrodes, respectively. The first electrode was also connected to the ground terminal on the other side of the PLZT wafer. An alternative contact was made for each of the devices at the half way point of the active area. This allows the use of half the active area, i.e. $1.5\text{mm} \times 3\text{mm}$ so that the beam steering angle doubles with the same external voltage, or the applied voltage is reduced for the same steering requirement.

5. Mathematical description of the electro-optic process

The mathematical expression of the electro-optic effect inside the PLZT substrate is as follows. First of all, we define the coordinate system. Principal axes x and z lie in the top surface of the PLZT and are perpendicular and parallel to the electrodes, respectively. Axis y points into the PLZT wafer. Thus the boundary conditions for the voltage distribution inside the PLZT substrate are given by

$$V(x, y)|_{x=0} = 0, \tag{13}$$

$$V(x, y)|_{y=t} = 0, \text{ and} \tag{14}$$

$$V(x, y)|_{y=0} = \begin{cases} 0, & 0 \leq x < d, \\ \frac{x-a}{d} V_1, & d \leq x < p \\ V_1, & p \leq x < p+d \\ V_1 + \frac{x-p-d}{d} (V_2 - V_1), & p+d \leq x < 2p \\ V_2, & 2p \leq x < 2p+d, \\ \dots \\ V_{N-1} + \frac{x-W'+p}{d} (V_N - V_{N-1}), & W'-p \leq x < W'-d \\ V_N, & W'-d \leq x < W', \end{cases} \quad (15)$$

with $p=d+a$ and $W'=Np+d$. Note that the W' here is not the W in the main text which is equal to Np . From the boundary condition at $x=0$ and assuming a periodic property, the solution for the voltage distribution inside the PLZT substrate has the following sine expansion form

$$V(x, y) = \sum_{n=1}^{\infty} \sin(\xi_n x) [A(\xi_n) \exp(\xi_n y) + B(\xi_n) \exp(-\xi_n y)], \quad (16)$$

where $A(\xi_n)$ and $B(\xi_n)$ are corresponding coefficients for the ξ_n harmonic component and

$$\xi_n = \frac{n\pi}{2W'}. \quad (17)$$

Because of the boundary condition at $y=t$, the general solution becomes

$$V(x, y) = \sum_{n=1}^{\infty} \sin(\xi_{2n-1} x) P(\xi_{2n-1}) \frac{\sinh[\xi_{2n-1}(t-y)]}{\sinh(\xi_{2n-1} t)}, \quad (18)$$

where $P(\xi_n)$ is the Fourier component, which can be given by

$$P(\xi_n) = \frac{2}{W'} \int_0^{W'} V(x, y)|_{y=0} \sin(\xi_n x) dx. \quad (19)$$

Even numbered components, ξ_{2n} , do not appear in the sine expansion due to normalization. The electrical field distributions can be obtained by taking the gradient of the above voltage distribution as given by

$$E_x(x, y) = -\frac{\partial V(x, y)}{\partial x} = -\sum_{n=1}^{\infty} \xi_{2n-1} \cos(\xi_{2n-1} x) P(\xi_{2n-1}) \frac{\sinh[\xi_{2n-1}(t-y)]}{\sinh(\xi_{2n-1} t)}, \text{ and} \quad (20)$$

$$E_y(x, y) = -\frac{\partial V(x, y)}{\partial y} = \sum_{n=1}^{\infty} \xi_{2n-1} \sin(\xi_{2n-1} x) P(\xi_{2n-1}) \frac{\cosh[\xi_{2n-1}(t-y)]}{\sinh(\xi_{2n-1} t)}. \quad (21)$$

From the above equations, the electrical field and its direction with respect to the y axis can be determined by

$$E(x, y) = \sqrt{E_x^2(x, y) + E_y^2(x, y)}, \text{ and} \quad (22)$$

$$\theta(x, y) = \cos^{-1} \left\{ \frac{E_y(x, y)}{E(x, y)} \right\}. \quad (23)$$

Taking a coordinate transform in the x - y plane with the field direction as the new x' axis and the one simultaneously perpendicular to x' and z as new y' , the new principal axes of the index ellipsoid of the PLZT at an arbitrary location inside the wafer are expressed as

$$n_{x'}(x, y) = n_0 - \frac{1}{2} n_0^3 R_{11} E^2(x, y), \quad (24)$$

$$n_{y'}(x, y) = n_0 - \frac{1}{2} n_0^3 R_{12} E^2(x, y), \text{ and} \quad (25)$$

$$n_z(x, y) = n_0 - \frac{1}{2} n_0^3 R_{12} E^2(x, y), \quad (26)$$

where x' , y' and z denote the new coordinates. The index of refraction for the z -polarized light, whose polarization is parallel to the electrodes, is $n_z(x, y)$. The refractive index for the x -polarized light, whose polarization is perpendicular to the electrodes, is $n_x(x, y)$, which is given by the following relationship with the principal axes of index ellipsoid¹⁷

$$\frac{1}{n_x^2(x, y)} = \frac{\sin^2[\theta(x, y)]}{n_{x'}^2(x, y)} + \frac{\cos^2[\theta(x, y)]}{n_{y'}^2(x, y)}. \quad (27)$$

With the indices available, the phase modulation for the x - and z -polarized light can be written as

$$\phi_x(x) = \frac{2\pi}{\lambda} \int_0^x n_x(x, y) dy, \quad (28)$$

$$\phi_z(x) = \frac{2\pi}{\lambda} \int_0^x n_z(x, y) dy, \quad (29)$$

where λ is the laser wavelength. The transmitted light also experiences an intrinsic phase modulation by the ITO electrodes. ITO has a refractive index of 1.775. Therefore the 130nm thick ITO introduces an additional phase modulation of approximately $\pi/3$. The overetch during the electrode patterning increases this modulation. This modulation generates diffraction orders but does not influence the steering property of the device.

6. Experimental test of the device

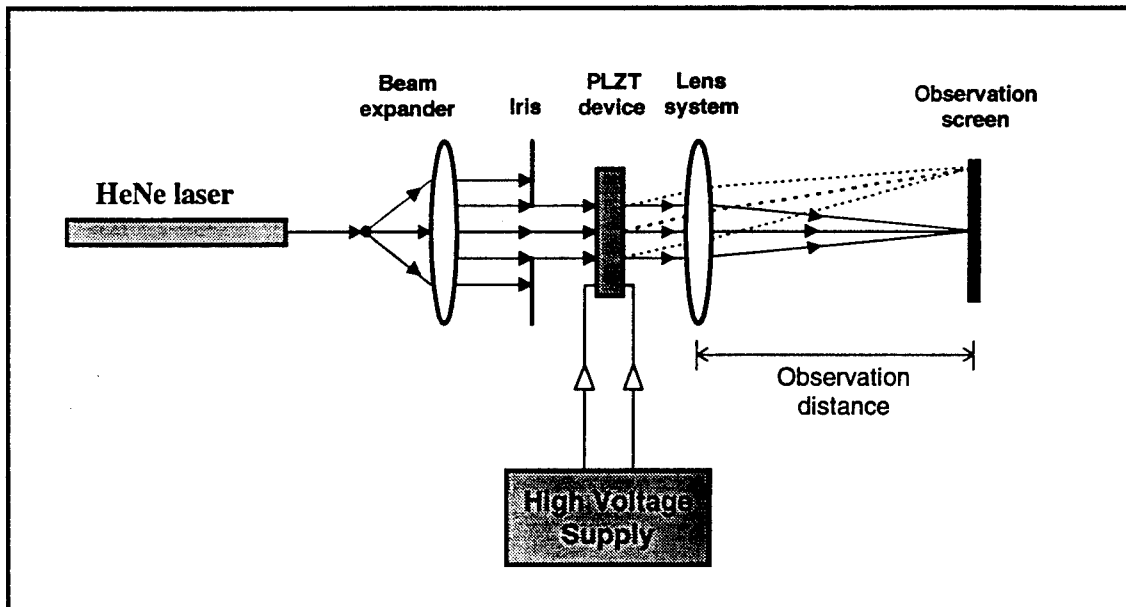
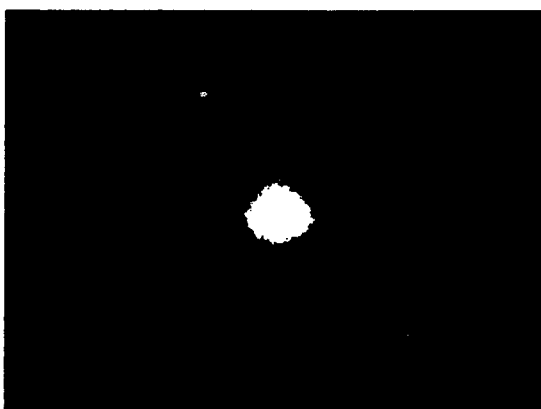


Figure 3. Experimental setup for the steering angle measurement.

To perform the experimental test, an experimental system was set up, as illustrated in Figure 3. A linearly polarized He-Ne laser beam of 633nm with its axis normal to the device surface was incident on the electro-optic steering device. The transmitted beam was examined at a certain distance behind the device. A high voltage power supply was used to generate a voltage of up to 700V. The electrical power consumption are 70 mW and 50 mW for the 40 μ m and 100 μ m period designs, respectively, at 700 V. A steering angle of 0.04°, which was in agreement with the prediction found by using Equation 10, was measured for both devices by comparing the light spot displacement and the observing distance. Steering angles of 0.03° and 0.02° were also obtained for 600V and 500V, respectively. The angle was quite small for an applied voltage below 400V because of the quadratic relationship between the steering angle and the applied voltage as given by Equation 10. Figure 4 gives the far field diffraction patterns of the laser beam for the 100 μ m period device taken without the presence of the device, with the device but no applied voltage and with the device with an applied voltage of 600V, respectively. The result shows that the beam quality was not obviously affected by the introduction of the device and the applied voltage.



(a)



(b)



(c)

Figure 4. Far field patterns of laser beam passing through the 100 μm period device a) without the device, b) with the device but without applied voltage, and c) with an applied voltage of 600 V, respectively.

Experimental tests on both of the designs were conducted. There is no obvious difference of the performance between these two designs, except the electrical power consumption. This can be verified by the voltage distribution inside the PLZT substrate. A simulated voltage distribution is illustrated in Figure 5. It can be seen that the voltage changes smoothly in most of the PLZT cross-section except the place near the electrodes. When the electrode period changes in some range, the voltage will change a little at the place near the electrodes and remain relatively the same elsewhere. Thus the two designs in the fabrication basically behave alike.

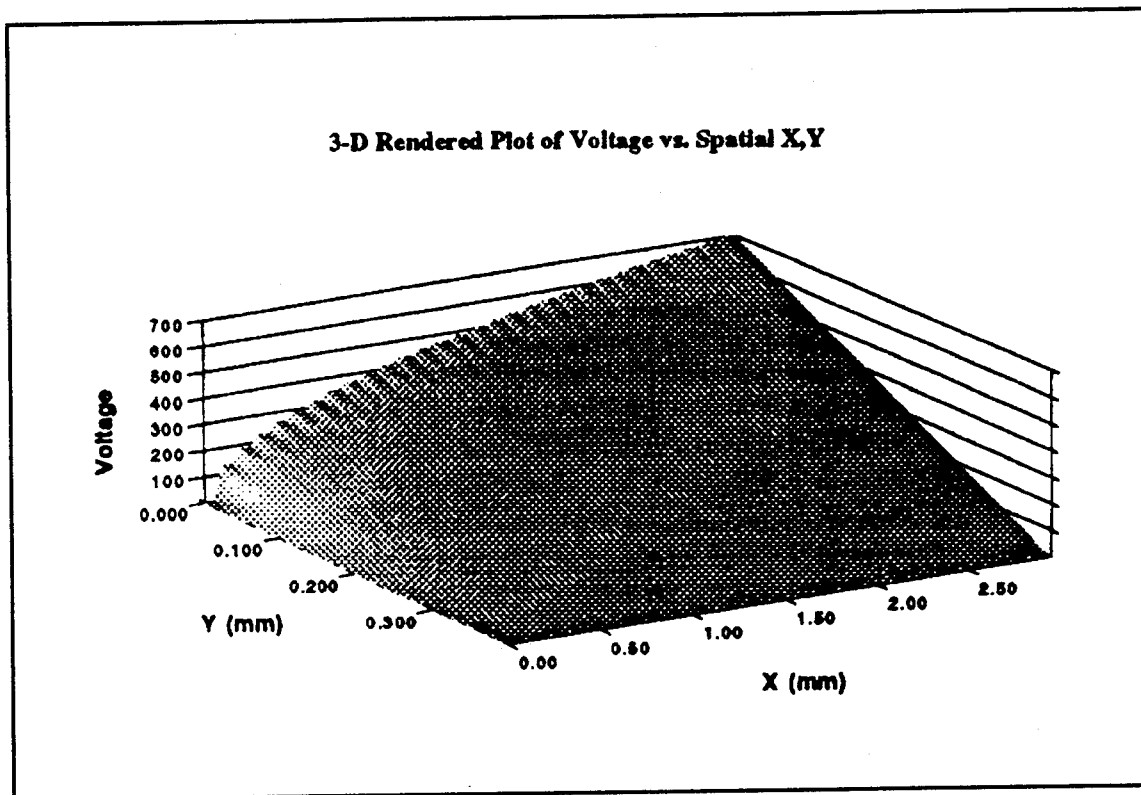


Figure 5. Calculated voltage distribution inside PLZT; (x,y) indicates the coordinate of the plane perpendicular to the electrodes with x on the PLZT top surface.

Experimental observation also showed that there was no significant difference between the two cases where the field polarization of the incident beam was parallel and perpendicular to the electrodes' orientation, respectively. This suggests that the electrical field resulting from the inter-electrode voltage difference has little influence on the overall field distribution in PLZT. In other words, the resultant index ellipsoid is an ellipsoid of revolution with its axis perpendicular to substrate surfaces. This is understandable if we look into the device structure again in Figure 1. The thickness of the PLZT substrate is comparable to the electrode period. The electrical field in PLZT substrate mainly contains two induced components, one is between the specific electrode and the ground, the other is from the voltage difference between this electrode and its neighbor electrodes. In most cases the first component is much larger than the second one because $V_k \gg V_k - V_{k-1}$ for a moderated or large k . In addition, the first component remains roughly uniform along the depth of the substrate while the second component exists mainly near the top surface of the substrate. As a result, the index modulation and thus the phase modulation are mainly due to the effect of the first electrical field component which is along the light path. This property can be confirmed by the computer simulation in the next section. This polarization-independent property of the electro-optic beam steering device may be useful in some practical applications.

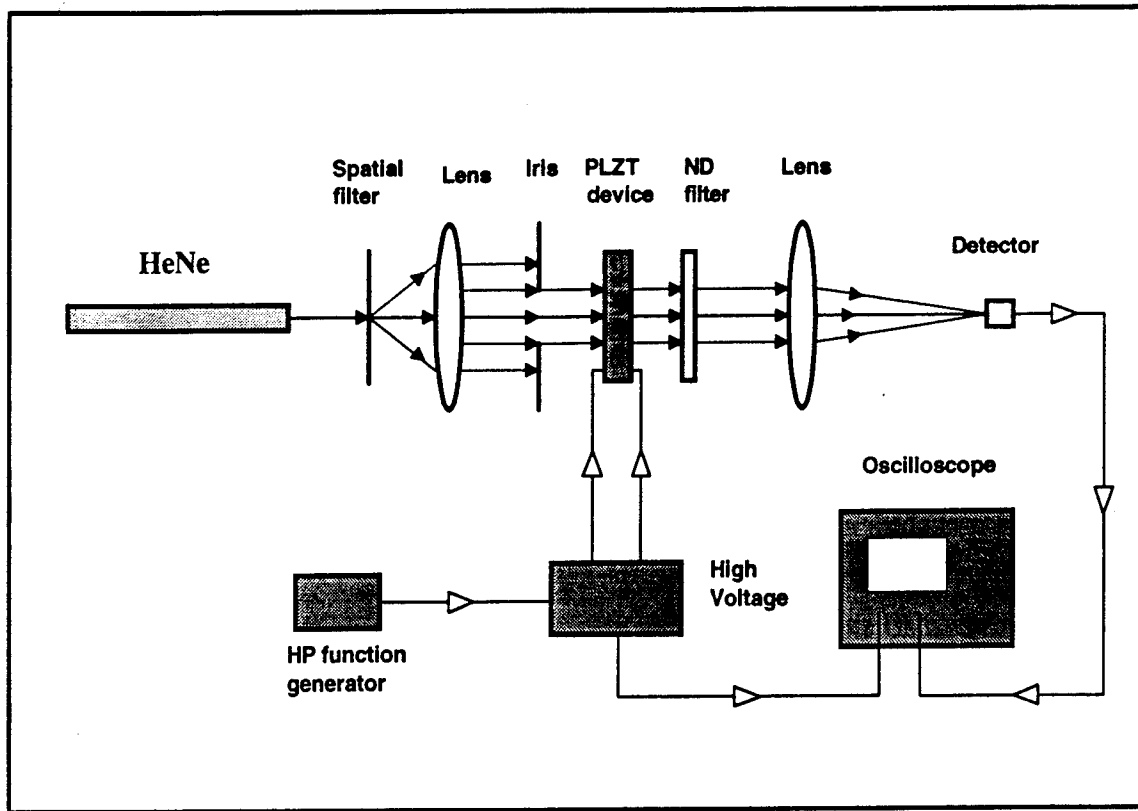
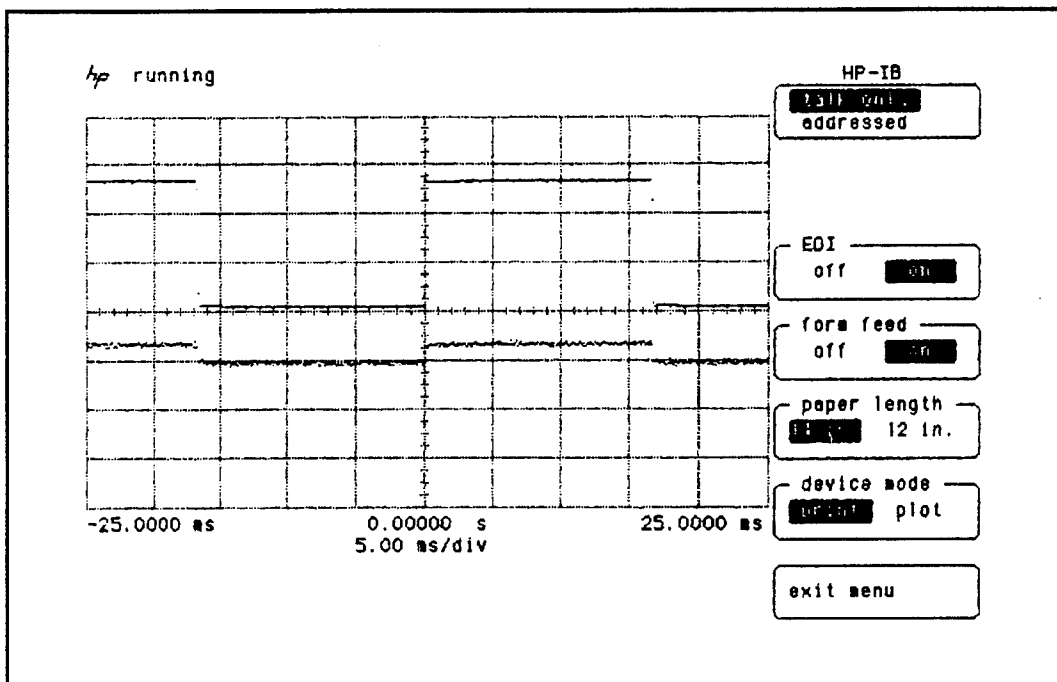


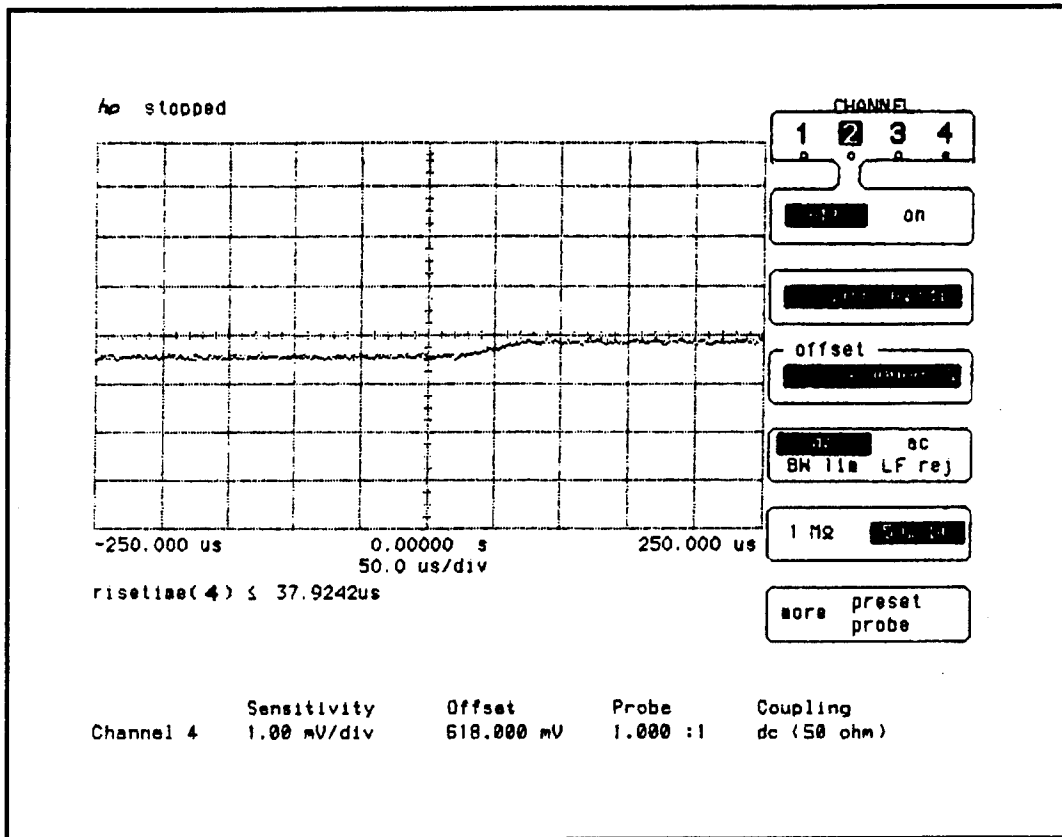
Figure 6. Setup utilized to measure the response time of the device.

Time response is an important parameter for an electro-optic device. The setup to measure the response time is shown in Figure 6. The experiment was performed on the 100 μm period device. The device was driven by a high voltage supply which was modulated by a square wave function supplied by a Hewlett Packard 8116A pulse function generator. At 500V and a frequency of 30Hz, the rise time was measured to be 37.92 μs on a Hewlett Packard 54503H digital oscilloscope. This result was obtained by comparing the output of the voltage supply and the device's output, which are simultaneously displayed on the oscilloscope, as shown in Figure 7. Figure 7(a) shows the square wave voltage signal and the optical beam response measured. When the time

dimension is expanded as shown in Figure 7(b), we can see the beam response. PLZT itself has an intrinsic time response less than $1\mu\text{m}$, and the time response of the device depends mainly on the value of the resistance of the resistors and the parasitic capacitance among the electrodes and the ground terminal. We believe that this time response can be shortened by better device lay-out and better material for the electrodes in order to reduce the RC constant.



(a)



(b)

Figure 7. Measured time response of the device when a square wave voltage was applied.

7. Computer simulation

A computer simulation was generated for the 100 μ m period design for comparison with and verification of the experimental test. We followed the complete physical principles for the electro-optic effect of the quadratic PLZT ceramic in the simulation and determined the field distribution inside the PLZT by applying boundary conditions^{13,17} as shown in Equations 13-15. To ease the mathematical derivation and make use of the

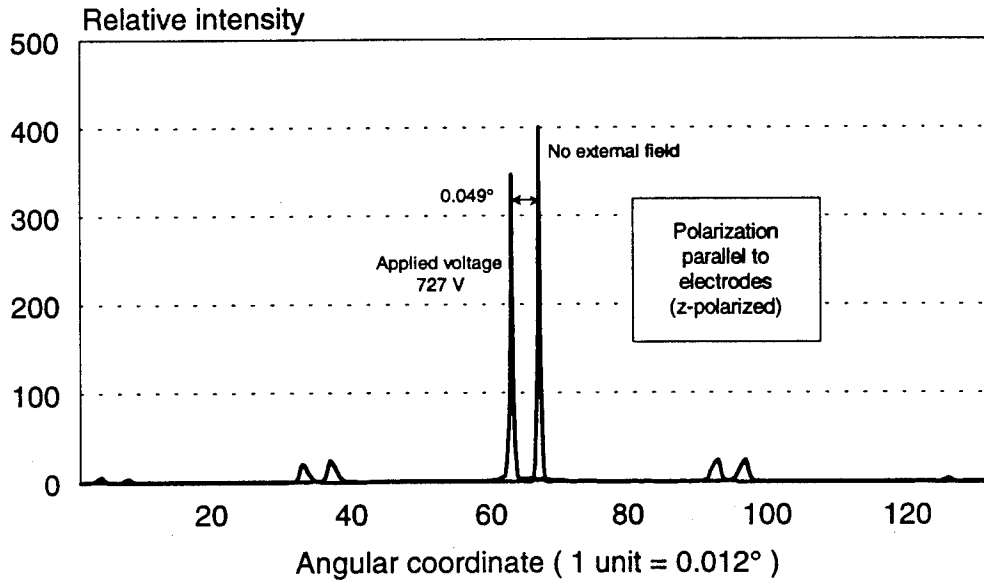
digital fast Fourier transform (FFT) the voltage distribution was periodically expanded such that

$$V(x + 4mW', y) = V(x, y), \quad (30)$$

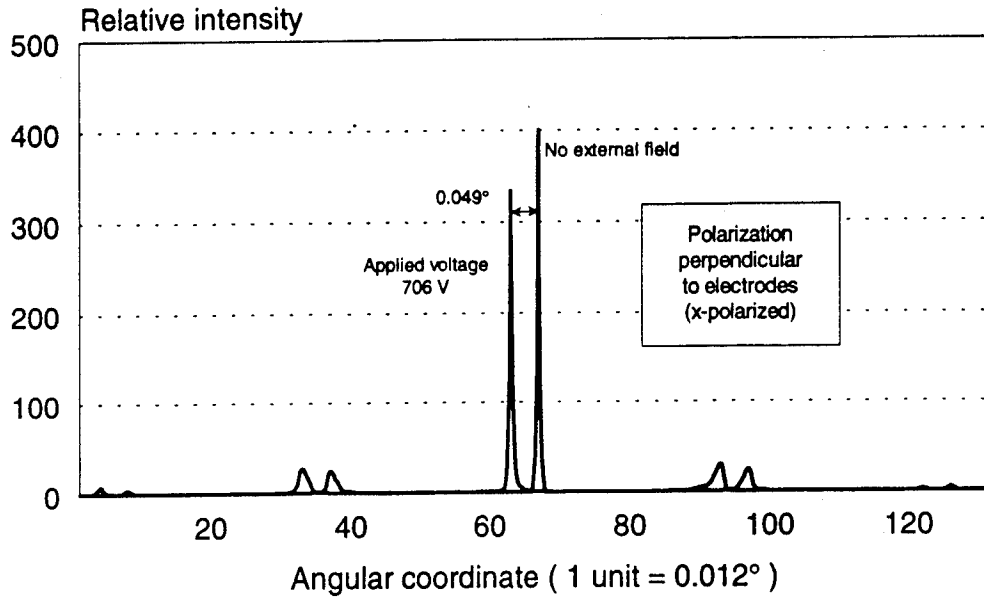
$$V(x + (4m + 1)W', y) = V(W' - x, y), \text{ and} \quad (31)$$

$$V(x + (4m + 2)W', y) = -V(x, y), \quad (32)$$

where m is an integer. This assumption assures that the potential along the $x=0$ line is absolutely zero and that along $x=W'$ is the maximum as compared with corresponding values along $x < W'$. The 130nm thick ITO electrodes form an intrinsic binary phase grating with modulation of 0.33π . A 512 point FFT was employed to obtain the far field angular spectra produced by the combined phase modulation inside the PLZT and the ITO electrodes.



(a)



(b)

Figure 8. Simulated far field diffraction with and without an applied voltage for the light with polarization (a) parallel and (b) perpendicular to the electrode orientation.

Figure 8 gives the far field distribution with and without the external voltage, respectively. A 0.049° steering angle occurred at an applied voltage of 706V for x-polarized light and of 727V for z-polarized light. The main lobe of this simulated far field diffraction agrees with the experimental result. However, the fabricated device has a stronger high order diffraction which resulted from the over etching of the PLZT substrate during the electrode etching process. This figure shows that there is no significant difference between these two polarization, which is in agreement with the experimental observation. Figure 9 demonstrates the computed relationship between the steering angle and the applied voltage. Experimental data are also plotted for comparison. The experimental results show that the quadratic coefficient of the material we used is

less than the data introduced in Section 2. Values of the quadratic coefficient of PLZT 9/65/35 diverge greatly from report to report.²³ In some cases, the coefficient is much larger than the one we used. We believe that with proper selection of materials, the working voltage can be dramatically decreased.

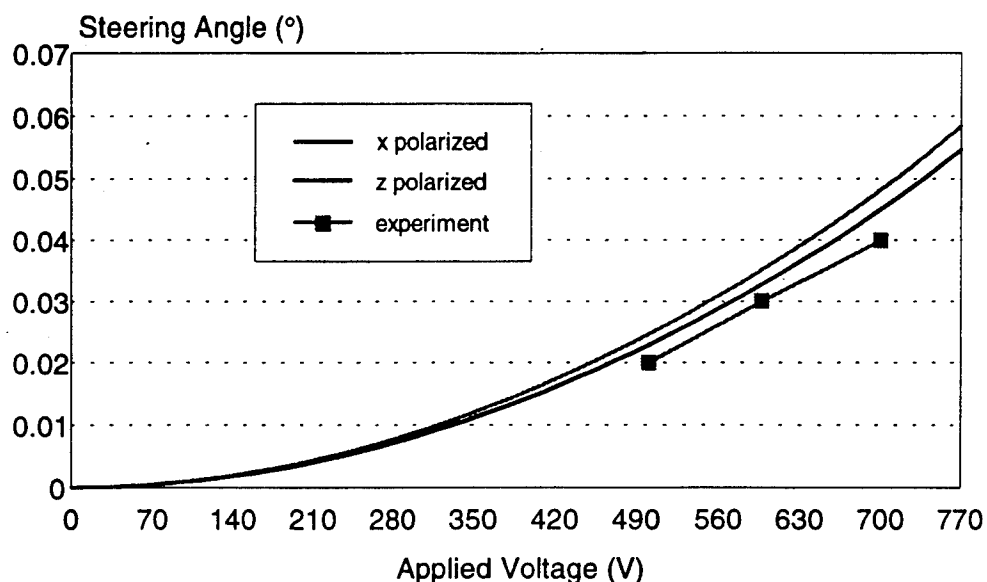


Figure 9. Comparison of experimental and simulated relationships between the applied voltage and the steering angle.

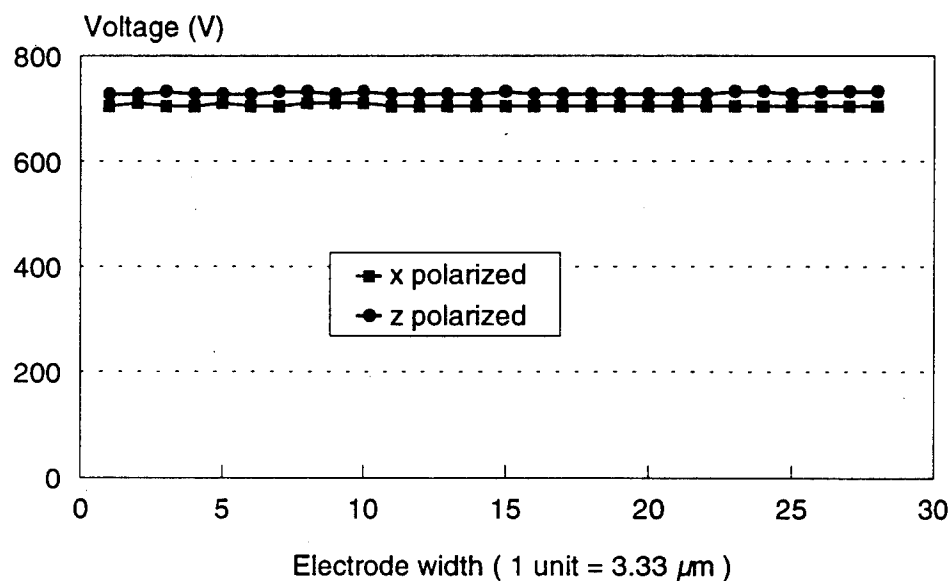


Figure 10. Simulated voltage dependence on the electrode width for the case that the steering angle is fixed to 0.04° .

While keeping the electrode period unchanged, the dependence of the required scan voltage for a given steering angle was calculated as a function of the electrode width. The effect of the electrode width on the required scan voltage is shown in Figure 10. The $100\mu\text{m}$ period was divided into 30 equal parts. The horizontal axis denotes the electrode width in terms of the parts. The ratio of the electrode width to the electrode spacing had almost no effect on the required voltage. The result can be explained by the following. When the electrode spacing is large, the transversal field component produced by the adjacent electrodes is weak and exists only at the region near the top surface of the substrate. When the spacing is narrow, the transversal field is comparably strong but exists in a very limited region. Thus its influence remains weak. This suggests that very thin opaque metal electrodes can be used instead of wide transparent ITO electrodes so as to decrease the resistance distributed on the electrodes. This change can simplify the fabrication and reduce the RC constant of the device. Of course, this result does not imply its validity for all the cases. When electrode spacing is comparably smaller than the substrate thickness, the transversal electrical field will have a strong influence. It may change the properties claimed here.

Far field beam quality was computationally shown to be diffraction limited. The simulation of the beam quality demonstrated that the beam's divergent angle remains unchanged as different scan voltages are applied, in agreement with our experimental observation shown in Figure 4. The half intensity width of the zero diffraction order is

0.015°. Diffraction calculations give the diameter of the Airy disk to be about 0.029°. The corresponding half intensity width is 0.013°.

8. Discussions and conclusions

In conclusion, an optical steering device based on a substrate of PLZT ceramic has been presented. On-substrate resistors were fabricated by evaporating a less conductive metal, and the resistance was controlled by varying the length of the metal film bar which connects two adjacent electrodes. A steering ability was experimentally demonstrated, which is in agreement with both the predicted estimation and the precise computer simulation. A fast time response and good beam quality were also observed. This device can have applications in laser disk tracking and/or fine alignment of board-to-board optical interconnections. To decrease the applied voltage, thin PLZT substrate with large quadratic electro-optic coefficients should be used. The steering range achieved by this design is relatively small but it is a continuous steering. When combined with a discrete steering device such as a blazed grating²⁰, a large steering range can be achieved.

References

1. W. Goltzos and M. Holz, "Agile beam steering using binary optical microlens arrays," *Opt. Eng.* **29**, 1392-1397 (1990).
2. Michael W. Farn, "Agile beam steering using phase-arraylike binary optics," *Appl. Opt.* **33**, 5151-5158 (1994).
3. C. L. M. Ireland and J. M. Ley, *Electrooptic Scanners* (Marcel Dekker, New York, 1991).
4. E. A. Watson, "Analysis of steering with decentered microlens arrays," *Opt. Eng.* **32**, 2665-2670 (1993).
5. E. A. Watson, P. F. McManamon, L. J. Barnes, and A. J. Carney, "Application of dynamic gratings to broad spectral band beam steering," in *Laser beam propagation and control*, Proc. Soc. Photo-Opt. Instrum. Eng. **2120**, 178-185 (1994).
6. E. A. Watson and L. J. Barnes, "Optical design considerations for agile beam steering," in *Laser beam propagation and control*, Proc. Soc. Photo-Opt. Instrum. Eng. **2120**, 186-193 (1994).
7. R. M. Matic, "Blazed phase liquid crystal beam steering," in *Laser beam propagation and control*, Proc. Soc. Photo-Opt. Instrum. Eng. **2120**, 194-205 (1994).
8. T. Utsunomiya, "Optical deflector with tandem electrodes using PLZT ceramic," *Jpn. J. Appl. Phys. Suppl.* **28**, 164-166 (1989).
9. R. A. Meyer, "Optical beam steering using a multichannel lithium tantalate crystal," *Appl. Opt.* **11**, 613-616 (1972).

10. Yuichi Ninomiya, "Ultrahigh resolving electrooptic prism array light deflectors," *IEEE J. Quantum Electron.* **QE-9**, 791-795 (1973).
11. Gordon D. Love, John V. Major, and Alan Purvis, "Liquid-crystal prisms for tip-tilt adaptive optics," *Opt. Lett.* **19**, 1170-1172 (1994).
12. H. Sato, T. Tatebayashi, T. Yamamoto, and K. Hayashi, "Electro-optic lens composed of transparent electrodes on PLZT ceramic towards optoelectronic devices," in *Optics in complex systems*, F. Lanzl, H. Preuss, and G. Weigolt, eds., *Proc. Soc. Photo-Opt. Instrum. Eng.* **1319**, 493-494 (1990).
13. Tsuyoshi Tatebayashi, Takashi Yamamoto, and Heihachi Sato, "Electro-optic variable focal-length lens using PLZT ceramic," *Appl. Opt.* **30**, 5049-5055 (1991).
14. Tsuyoshi Tatebayashi, Takashi Yamamoto, and Heihachi Sato, "Dual focal point electrode-optic lens with a Fresnel-zone plate on a PLZT ceramic," *Appl. Opt.* **31**, 2770-2775 (1992).
15. K. Nagata and H. Honma, "Properties of PLZT shutter with copper plating electrodes," *Jpn. J. Appl. Phys. Suppl.* **28**, 167-169 (1989).
16. T. Utsunomiya, "Optical switch using PLZT ceramics," *Ferroelectrics*, **109**, 235-240 (1990).
17. Q. Wang Song, Pierre J. Talbot, and Joanne H. Maurice, "PLZT based high-efficiency electro-optic grating for optical switching," *J. Mod. Opt.* **41**, 717-727 (1994).
18. P. J. Talbot and Q. W. Song, "Design and simulation of PLZT-based electrooptic phased array scanners," *Optical Memory and Neural Networks*, **3**, 111-117 (1994).

19. Pierre J. Talbot, "Design and simulation of PLZT-based scanning grating lobe optical array generators," *Opt. Commun.* **113**, 378-384 (1995).
20. James A. Thomas and Yeshaiahu Fainman, "Programmable diffractive optical element using a multichannel lanthanum-modified lead zirconate titanate phase modulator," *Opt. Lett.* **20**, 1510-1512 (1995).
21. Nabeel A. Riza and Michael C. DeJule, "Three-terminal adaptive nematic liquid-crystal lens device," *Opt. Lett.* **19**, 1013-1015 (1994).
22. G. H. Haertling, "PLZT electrooptic ceramics and devices," in *Industrial Applications of Rare Earth Elements*, K. A. Gschneidner, Jr. Ed., ACS Symposium Series, **164**, 265-283 (1981).
23. Dennis H. Goldstein, "PLZT modulator characterization," *Opt. Eng.* **34**, 1589-1592 (1995).

***MISSION
OF
ROME LABORATORY***

Mission. The mission of Rome Laboratory is to advance the science and technologies of command, control, communications and intelligence and to transition them into systems to meet customer needs. To achieve this, Rome Lab:

- a. Conducts vigorous research, development and test programs in all applicable technologies;
- b. Transitions technology to current and future systems to improve operational capability, readiness, and supportability;
- c. Provides a full range of technical support to Air Force Materiel Command product centers and other Air Force organizations;
- d. Promotes transfer of technology to the private sector;
- e. Maintains leading edge technological expertise in the areas of surveillance, communications, command and control, intelligence, reliability science, electro-magnetic technology, photonics, signal processing, and computational science.

The thrust areas of technical competence include: Surveillance, Communications, Command and Control, Intelligence, Signal Processing, Computer Science and Technology, Electromagnetic Technology, Photonics and Reliability Sciences.